
000 UNSUPERVISED ORDERING FOR MAXIMUM CLIQUE

001

002

003 **Anonymous authors**

004 Paper under double-blind review

006 007 ABSTRACT

009 We propose an unsupervised approach for learning vertex orderings for the maximum
010 clique problem by framing it within a permutation-based framework. We
011 transform the combinatorial constraints into geometric relationships such that the
012 ordering of vertices aligns with the clique structures. By integrating this clique-
013 oriented ordering into branch-and-bound search, we improve search efficiency and
014 reduce the number of computational steps. Our results demonstrate how unsu-
015 pervised learning of vertex ordering can enhance search efficiency across diverse
016 graph instances. We further study the generalization across different sizes.

018 1 INTRODUCTION

020 Unsupervised Learning (UL) is an emerging paradigm for solving Combinatorial Optimization
021 (CO) problems. While Supervised Learning (SL) requires expensive labelled data, and Reinforce-
022 ment Learning (RL) struggles with sparse rewards and high training variance, leading to unstable
023 performance, UL offers a promising alternative Min et al. (2023).

025 The Maximum Clique Problem (MCP) is of fundamental importance in graph theory and combi-
026 natorial optimization, with significant theoretical and practical implications. Formally, given an
027 undirected graph $G(V, E)$, where V is the set of vertices and E is the set of edges, the MCP seeks the
028 largest subset $C \subseteq V$ such that $\forall u, v \in C, \{u, v\} \in E$. In other words, the induced subgraph $G[C]$
029 is a complete graph, and the goal is to maximize $|C|$, the cardinality of the clique. **MCP is not only**
030 **NP-hard but also hard to approximate, since no $O(n^{1-\varepsilon})$ -approximation is possible unless $P = NP$**
031 Engebretsen and Holmerin (2000); Khot (2001); Zuckerman (2006). The MCP has wide-ranging
032 applications, including social network analysis, where it helps uncover tightly connected communities,
033 and bioinformatics, where it is used to identify dense clusters in protein interaction networks Bomze
034 et al. (1999).

035 Exact algorithms for the MCP primarily follow the branch-and-bound framework. Among these,
036 a common strategy is to color the vertices in a specific order for computing upper bounds and
037 guiding vertex selection Tomita and Seki (2003); Tomita et al. (2010); San Segundo et al. (2011);
038 Konc and Janezic (2007). Other methods include iterative deepening with sub-clique information,
039 or use MaxSAT-based bounding Wu and Hao (2015). However, these algorithms mainly rely on
040 hand-crafted features to design effective pruning rules and branching strategies. Recently, there
041 has been a paradigm shift towards data-driven approaches, where machine learning techniques are
042 employed to build efficient search strategies. Among these data-driven methods, UL shows particular
043 promise because it can leverage the inherent structural patterns in graphs without requiring expensive
044 labelled training data.

045 Several approaches have tackled the MCP using UL by framing it as a binary classification task Kar-
046 alias and Loukas (2020). Recent advances have focused on two key areas: developing more so-
047 phisticated graph neural network architectures and designing novel loss functions Karalias et al.
048 (2022). These approaches aim to learn a function $f_\theta : G(V, E) \rightarrow [0, 1]^n$ that maps an input graph
049 to vertex-level probabilities, optimizing the model to identify vertices that belong to the maximum
clique.

050 Here, we propose an alternative approach that learns vertex ordering rather than binary assignments
051 for MCP. **Graph vertex ordering is a foundational concept in combinatorial optimization on graphs,**
052 **including the MCP, where an appropriate vertex permutation can significantly influence the efficiency**
053 **of exact search algorithms. Traditional approaches often rely on hand-crafted heuristics, such as**
degree-based ordering Carraghan and Pardalos (1990); Tomita et al. (2010); San Segundo et al.

(2011); Jiang et al. (2017); Szabó and Zavalnij (2018). Recently, graph reordering has also attracted interest in the machine learning community, particularly for enhancing the efficiency of graph neural networks Arai et al. (2016); Balaji and Lucia (2018); Merkel et al. (2024). These studies highlight that suitable vertex permutations can substantially impact algorithmic performance—for example, by exposing dense substructures or minimizing irregular memory access patterns.

Consider the graph and its matrix representations shown in Figure 1. Our goal is to identify potential cliques by reordering vertices. Given a graph with n nodes and adjacency matrix $A \in \mathbb{R}^{n \times n}$, the matrix $\mathbf{M}(A) = J - I - A$ represents non-adjacent vertex pairs with 1s and adjacent pairs with 0s, where $J \in \mathbb{R}^{n \times n}$ is the all-ones matrix and $I \in \mathbb{R}^{n \times n}$ is the identity matrix, $\mathbf{M}(A)$ is the adjacency matrix of the complement graph.

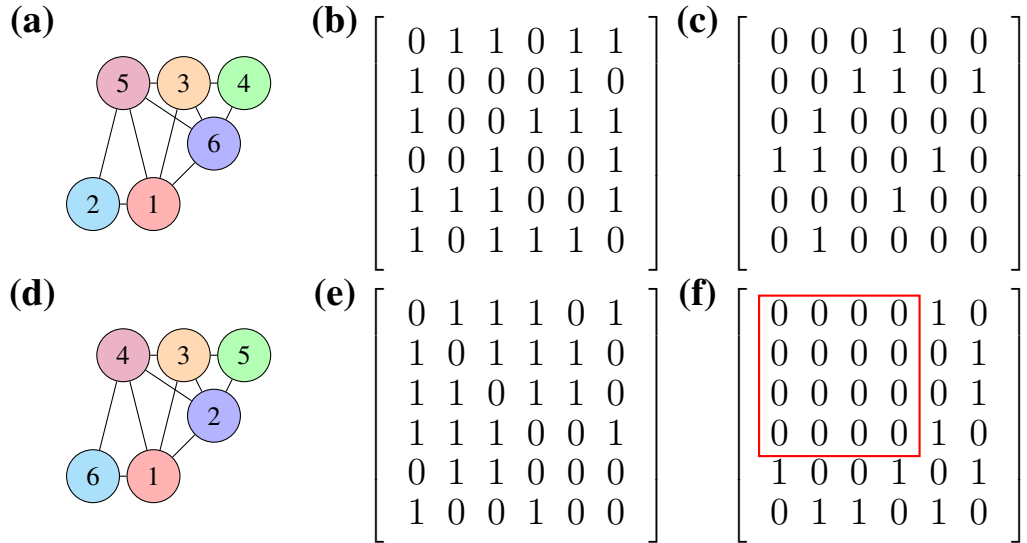


Figure 1: Graph representations and their corresponding matrices. (a) The original graph, (b) the corresponding adjacency matrix A , (c) $\mathbf{M}(A) = J - I - A$ (where J is the all-ones matrix and I is the identity matrix); (d) graph (a) with reordered nodes, (e) the corresponding adjacency matrix A' , (f) $\mathbf{M}(A') = J - I - A'$.

Now, consider the two different vertex orderings illustrated in Figure 1 (a) and (d). Their corresponding adjacency matrices, denoted as A and A' , are shown in Figure 1 (b) and (e). The matrices $\mathbf{M}(A)$ and $\mathbf{M}(A')$ are presented in Figure 1 (c) and (f), respectively. In $\mathbf{M}(A')$, adjacent vertices (represented by 0s) are successfully clustered in the upper-left corner, as highlighted by the red box. This clustering effectively reveals potential clique members, since vertices within a clique must be adjacent to each other, corresponding to the concentrated region of 0s in $\mathbf{M}(A')$. Thus, if we can find an optimal vertex ordering that places the clique nodes at the front, the clique structures will be revealed by the concentrated pattern of 0s in the transformed matrix $\mathbf{M}(A')$.

The reordering can be formally expressed as $\mathbf{M}(A') = \mathbf{P}^T \mathbf{M}(A) \mathbf{P}$, where $\mathbf{P} \in \mathbb{R}^{n \times n}$ is a permutation matrix. This formulation allows us to optimize the ordering of the vertices directly through a permutation matrix \mathbf{P} , from which we can extract the ordering of the vertices in the maximum clique. This permutation framework fundamentally differs from previous UL approaches. While previous methods encode clique constraints as penalty terms for binary classification, learning node-level probabilities, our framework learns relative node orderings that reveal clique structures. This shift from local classification (binary classification) to global structural relationships (ordering) enables the direct capture of inter-node correlations through permutation patterns.

In this paper, we transform the discrete combinatorial problem into a continuous geometric optimization using Chebyshev-based distances, which allows the model to capture clique structural relationships between nodes. We integrate UL with branch-and-bound algorithms, resulting in improved computational efficiency, especially for large, dense graphs. Our method is able to generalize across sizes, with inference overhead diminishing as graph size increases and outperforming tradi-

108
109
110
111
112
113
114
115
116
117
118
119
120
121
122
123
124
125
126
127
128
129
130
131
132
133
134
135
136
137
138
139
140
141
142
143
144
145
146
147
148
149
150
151
152
153
154
155
156
157
158
159
160
161

tional degree-based ordering. Our approach extends beyond binary classification, revealing how UL can learn fundamental combinatorial structures, suggesting broader applications in CO.

2 BACKGROUND

Branch-and-Bound for Maximum Clique The branch-and-bound (BnB) approach has been one of the most effective exact methods for solving MCP, with its performance largely determined by two key components: the vertex selection strategy and the upper bound computation. The algorithm incrementally constructs a clique by recursively selecting vertices while leveraging bounds to prune infeasible branches. A crucial factor in its efficiency is the use of heuristics such as *degree-based vertex ordering and coloring-based bounds*, which have been widely adopted in BnB frameworks San Segundo et al. (2011); Tomita and Seki (2003); Konc and Janezic (2007); Li et al. (2017). These techniques—ranging from greedy coloring bounds to efficient vertex selection—have significantly influenced subsequent advances McCreesh and Prosser (2013); San Segundo et al. (2016).

Unsupervised Learning for Vertex Ordering The most relevant UL work on graph ordering for combinatorial optimization is UL for Travelling Salesman Problem (TSP), as explored by Min and Gomes (2023); Min et al. (2023). The goal of TSP is to find the shortest Hamiltonian cycle. Min and Gomes (2023) use a Graph Neural Network (GNN) to construct a soft permutation matrix $\mathbb{T} \in \mathbb{R}^{n \times n}$ and optimize the following loss:

$$\mathcal{L}_{\text{TSP}} = \langle \mathbb{T} \mathbb{V} \mathbb{T}^T, \mathbf{D}_{\text{TSP}} \rangle, \quad (1)$$

where \mathbb{V} represents a Hamiltonian cycle from node $1 \rightarrow 2 \rightarrow \dots \rightarrow n \rightarrow 1$, and \mathbf{D}_{TSP} is the distance matrix with self-loop distances set as λ . Here, a soft permutation matrix is a *doubly stochastic* matrix, meaning that every entry satisfies $\mathbb{T}_{ij} \geq 0$ and both its row and column sums are equal to 1, that is,

$$\sum_{j=1}^n \mathbb{T}_{ij} = 1 \quad \text{and} \quad \sum_{i=1}^n \mathbb{T}_{ij} = 1 \quad \text{for all } i, j. \quad (2)$$

Such matrices provide a continuous relaxation of discrete permutation matrices, enabling gradient-based optimization while still approximating valid permutations. Since the Hamiltonian cycle constraint holds under any permutation and the order is equivalent with respect to the permutation, optimizing Equation 1 serves as a proxy for solving the TSP, incorporating both the shortest path and Hamiltonian cycle constraints. In other words, the order of vertices in the Hamiltonian cycle is determined by the permutation matrix and we aim to find the one that minimizes the total distance.

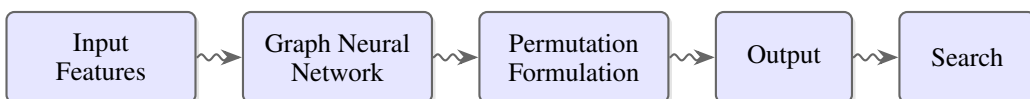


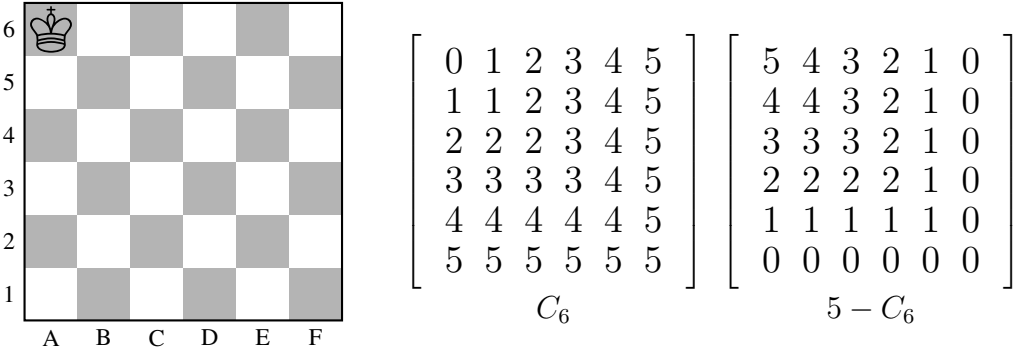
Figure 2: Overview of the unsupervised learning framework for TSP. The model takes graph features as input and processes them through a GNN. The objective is formulated within a permutation framework. The output provides a heat map that guides the subsequent search.

To learn the soft permutation matrix \mathbb{T} , Min and Gomes (2023) use a GNN coupled with a Gumbel-Sinkhorn operator. The transformation $\mathbb{T} \mathbb{V} \mathbb{T}^T$ is a heat map representation that guides the subsequent search procedure, as shown in Figure 2.

3 MODEL

In our model, the intuition and motivation are straightforward: we aim to learn a good vertex ordering to enhance BnB search performance for MCP. As mentioned in Figure 1, an effective ordering can reveal the hidden clique structure. While most existing search algorithms rely on degree-based vertex ordering, we propose incorporating a *clique-oriented* vertex ordering to guide the search process.

162 **Learning** We train our model to learn and generate *clique-oriented* ordering following the TSP
 163 framework, as illustrated in Figure 2. Our goal is to design a cost matrix $\mathbf{D}_{\text{Clique}}$ analogous to \mathbf{D}_{TSP}
 164 that transforms the discrete constraint satisfaction problem into a continuous geometric optimization.
 165 This transformation requires $\mathbf{D}_{\text{Clique}}$ to guide the vertices’ reordering process, with the specific aim
 166 of clustering vertices in a way that reveals potential clique structures.
 167



180 Figure 3: (a): Visualization of a 6x6 chessboard with a king positioned at A6; (b) the Chebyshev
 181 distance matrix C_6 , where each element represents the minimum number of moves required for a
 182 king to travel between corresponding squares; (c) $\bar{C}_6 = 5 - C_6$, where the elements at top left have
 183 larger weights. $C_n[i, j] = \max\{i, j\} - 1$ and $\bar{C}_n[i, j] = n - 1 - C_n = n - \max\{i, j\}$

184
 185 The key insight of our approach is to reorder vertices such that adjacent pairs are concentrated in
 186 specific regions of the matrix. This geometric perspective naturally leads to the Chebyshev distance
 187 matrix C_n and its complement \bar{C}_n , as illustrated in Figure 3. The Chebyshev distance is defined as
 188 the minimum number of moves a king piece requires to traverse a chessboard between two squares.
 189 For an $n \times n$ grid, we formalize this distance as $C_n[i, j] = \max\{i, j\} - 1$, with its complement
 190 $\bar{C}_n[i, j] = n - \max\{i, j\}$ assigning larger weights to elements in the upper-left region.

191 The Chebyshev distance matrix is crucial for our model to learn clique structures, as it will naturally
 192 guide the optimization to push adjacent vertex pairs (0 in $J - I - A$) toward the upper-left corner, ef-
 193 fectively clustering potential clique members together. Furthermore, we can strengthen this geometric
 194 intuition by exponentially scaling the distance weights. Specifically, when we set $\mathbf{D}_{\text{Clique}} = (n^2)^{\bar{C}_n}$,
 195 minimizing $\mathcal{L}_{\text{Clique}}(P) = \langle \mathbf{P}^T (J - I - A) \mathbf{P}, \mathbf{D}_{\text{Clique}} \rangle$ guarantees convergence to the optimal solution,
 196 where $\mathbf{P} \in S_n$ denotes a hard permutation matrix. In practice, we set $\mathbf{D}_{\text{Clique}} = (1 + \epsilon)^{(\bar{C}_n - n/2)}$,
 197 where ϵ is a positive constant. This formulation maintains the exponential weighting scheme and
 198 provides better numerical stability.

199 We train our neural network to minimize the clique-specific objective:
 200

$$\mathcal{L}_{\text{Clique}} = \langle \mathbb{T}^T (J - I - A) \mathbb{T}, \mathbf{D}_{\text{Clique}} \rangle, \quad (3)$$

201 where \mathbb{T} represents a soft permutation matrix.

202 While this formulation appears similar to the TSP objective in Equation 1, there is a difference in
 203 the matrix multiplication order. The TSP formulation uses $\mathbf{V} \mathbf{T} \mathbf{V}^T$, whereas our clique formulation is
 204 $\mathbb{T}^T (J - I - A) \mathbb{T}$. This distinction stems from different invariance requirements in the two problems.
 205 Let $\mathcal{H}_0 = \mathbb{T}_0 \mathbf{V} \mathbf{V}^T$ denote the initial heat map of TSP and \mathbb{T}_0 is the initial soft permutation matrix.
 206 For TSP, the permuted heat map should be equivariant under node reordering. When we apply a
 207 permutation matrix Π to the original node ordering, our GNN’s equivariance ensures $\mathbb{T} = \Pi \mathbb{T}_0$,
 208 resulting in a consistently transformed heat map $\Pi \mathcal{H}_0 \Pi^T$. **Equivariance here means that if we relabel**
 209 **the graph by Π , the output heat map should relabel in the same way, preserving the structure of the**
 210 **tour under any permutation of node indices.**

211 In contrast, for the maximum clique problem, $\mathbb{T}_0^T (J - I - A) \mathbb{T}_0$ must remain invariant under node
 212 reordering. When we apply a permutation Π , the $J - I - A$ transforms as $J - I - \Pi A \Pi^T$. Due to
 213 our GNN’s equivariance, $\mathbb{T} = \Pi \mathbb{T}_0$, making $(\Pi \mathbb{T}_0)^T (J - I - \Pi A \Pi^T) (\Pi \mathbb{T}_0)$ equal to the original

216 $\mathbb{T}_0^T(J - I - A)\mathbb{T}_0$. This invariance is crucial as we aim to reorder adjacent pairs in the upper-left
 217 corner, regardless of the initial vertex ordering.
 218

219 Overall, here we encode the MCP using the same framework as TSP, where discrete combinatorial
 220 constraints are transformed into continuous geometric optimization through matrix operations $\mathbb{T}\mathbb{V}\mathbb{T}^T$
 221 and $\mathbb{T}^T(J - I - A)\mathbb{T}$ with distance matrices \mathbf{D}_{TSP} and $\mathbf{D}_{\text{Clique}}$, respectively.
 222

223 **Search** As mentioned, *degree-based vertex ordering* and *coloring-based bounds* are widely adopted
 224 in BnB frameworks for solving the MCP Tomita and Seki (2003); Konc and Janezic (2007); Li and
 225 Quan (2010); San Segundo et al. (2011); Wu and Hao (2015); Li et al. (2017). Among these methods,
 226 MaxCliqueDynKonc and Janezic (2007), an improved version of Tomita et al.’s algorithm Tomita and
 227 Seki (2003), is a well-established exact solver that we adopt as our baseline to compare degree-based
 228 and UL-based vertex reordering methods. Most BnB methods for the MCP use the MaxCliqueDyn
 229 paradigm, which maintains a candidate set of vertices and recursively selects them based on degree or
 230 color to construct potential cliques while employing coloring-based bounds for pruning. Extensions
 231 such as MaxCliqueDyn+EFL+SCR Li and Quan (2010) integrate failed literal detection and soft
 232 clause relaxation but retain MaxCliqueDyn’s core structure.
 233

233 **Algorithm 1** MaxCliqueDyn: Maximum Clique Algorithm with Dynamic Upper Bounds

234 **Require:** Graph $G = (V, E)$, candidate set $R \subseteq V$, coloring C , depth *level*
 235 **Ensure:** Maximum clique in G

236 1: Initialize $Q \leftarrow \emptyset$, $Q_{max} \leftarrow \emptyset$, $S[level] \leftarrow 0$, $S_{old}[level] \leftarrow 0$ ▷ Cliques and steps
 237 2: $ALL_STEPS \leftarrow 1$, $T_{limit} \leftarrow 0.025$ ▷ Step counter and threshold
 238 3: Sort V in a non-increasing order with respect to their degrees; color first $\Delta(G)$ vertices ▷ Degree-based init coloring
 239 $1, \dots, \Delta(G)$, rest $\Delta(G) + 1$
 240 4: **procedure** MAXCLIQUEDyn($R, C, level$)
 241 5: $S[level] \leftarrow S[level] + S[level - 1] - S_{old}[level]$ ▷ Step count
 242 6: $S_{old}[level] \leftarrow S[level - 1]$ ▷ Save old count
 243 7: **while** $R \neq \emptyset$ **do**
 244 8: $p \leftarrow \arg \max_{v \in R} C(v)$ ▷ Best remaining vertex
 245 9: $R \leftarrow R \setminus \{p\}$ ▷ Remove vertex
 246 10: **if** $|Q| + C[\text{index_of_}p\text{_in_}R] > |Q_{max}|$ **then** ▷ Promising bound
 247 11: $Q \leftarrow Q \cup \{p\}$ ▷ Add to clique
 248 12: **if** $R \cap \Gamma(p) \neq \emptyset$ **then** ▷ Has neighbors, where $\Gamma(p)$ denotes the neighborhood of
 249 13: **vertex** p ▷ Near root
 250 14: **if** $S[level]/ALL_STEPS < T_{limit}$ **then** ▷ Better bounds
 251 15: Compute degrees in $G(R \cap \Gamma(p))$ ▷ Order by potential
 252 16: Sort $R \cap \Gamma(p)$ by non-increasing degree
 253 17: **end if** ▷ Color subgraph
 254 18: $C' \leftarrow \text{ColorSort}(R \cap \Gamma(p))$ ▷ Count step
 255 19: $S[level] \leftarrow S[level] + 1$ ▷ Update total
 256 20: $ALL_STEPS \leftarrow ALL_STEPS + 1$ ▷ Recurse
 257 21: MAXCLIQUEDyn($R \cap \Gamma(p), C', level + 1$)
 258 22: **else** ▷ New best
 259 23: **if** $|Q| > |Q_{max}|$ **then** ▷ Update max
 260 24: $Q_{max} \leftarrow Q$
 261 25: **end if**
 262 26: $Q \leftarrow Q \setminus \{p\}$ ▷ Backtrack
 263 27: **else** ▷ Prune branch
 264 28: **return**
 265 29: **end if**
 30: **end while**
 31: **end procedure**

267
 268 Building upon this representative model, we aim to learn vertex ordering directly from graph
 269 data to guide the BnB search, as an alternative to the traditional degree-based ordering used in
 MaxCliqueDyn.
 270

270 **MaxCliqueDyn** MaxCliqueDyn uses dynamic bound adjustment to efficiently solve the MCP. The
271 algorithm maintains two key sets: Q for the current growing clique and Q_{max} for the best solution
272 found. Step counters $S[level]$ and $S_{old}[level]$ track search progress.
273

274 The algorithm combines several optimization strategies: non-increasing degree ordering for initial
275 bounds, dynamic step counting for adaptive bound adjustment, and the `ColorSort` algorithm for
276 maintaining vertex ordering properties. By applying bound calculations selectively near the root
277 of the search tree, MaxCliqueDyn achieves significant performance improvements on dense graphs
278 while preserving efficiency on sparse instances Konc and Janezic (2007).
279

280 At the beginning, MaxCliqueDyn sorts vertices in non-increasing degree order and assigns the first
281 $\Delta(G)$ vertices colors 1 through $\Delta(G)$ and the remaining vertices color $\Delta(G) + 1$, where $\Delta(G)$ is
282 the maximum degree in G . This provides a computationally efficient starting point that supports the
283 algorithm's dynamic bound calculations throughout the search process Tomita and Seki (2003), the
284 algorithm is shown in Algorithm 1. This initial coloring strategy, though simple, establishes a valid
285 starting point for the BnB process. Rather than investing heavily in an optimal initial coloring, it uses
286 this basic coloring that improves automatically through the `ColorSort`. In practice, this simple
287 initial coloring achieves a balance between computation time and reduction in search space Tomita
288 and Seki (2003); Konc and Janezic (2007).
289

290 The `ColorSort` procedure plays a crucial role in the BnB framework by providing increasingly
291 refined upper bounds through an approximate graph coloring. Following Konc and Janezic (2007),
292 `ColorSort` first computes $k_{min} = |Q_{max}| - |Q| + 1$, which represents the minimum required
293 colors for potential improvements to the current best clique. It then assigns vertices to color classes
294 based on their adjacency relationships, where vertices receiving colors $k < k_{min}$ are maintained in
295 their original positions, while vertices with colors $k \geq k_{min}$ are reordered based on their assigned
296 colors, we refer more details to the MaxCliqueDyn paper Konc and Janezic (2007).
297

298 **From Soft Permutation \mathbb{T} to Hard Permutation \mathbf{P}** To transform the GNN output into a hard
299 permutation matrix \mathbf{P} , we employ a differentiable sorting operation. Specifically, we apply the
300 Gumbel-Sinkhorn operator to the GNN's output, which is a continuous relaxation of the permutation
301 during training while allowing us to obtain a hard permutation matrix during inference through the
302 Hungarian algorithm Mena et al. (2018). This permutation matrix \mathbf{P} is then used to reorder the input
303 vertices, partitioning likely clique nodes together.
304

305 In our GNN model, each node has two input features: (1) local density, calculated as the ratio of
306 existing edges to possible edges in the node's neighborhood, and (2) node degree. Our model first
307 generates logits which are transformed by a scaled tanh activation¹:
308

$$\mathcal{F} = \alpha \tanh(f_{GNN}(f_0, A)) \quad (4)$$

309 where $f_0 \in \mathbb{R}^{n \times 2}$ is the initial feature matrix and $A \in \mathbb{R}^{n \times n}$ is the adjacency matrix. The learned
310 features are transformed into logits which are scaled by tanh with factor α . These scaled logits
311 are then passed through the Gumbel-Sinkhorn operator to build a differentiable approximation of a
312 permutation matrix:
313

$$\mathbb{T} = GS\left(\frac{\mathcal{F} + \gamma \times \text{Gumbel noise}}{\tau}, l\right), \quad (5)$$

314 where γ is the scale of the Gumbel noise, τ is the temperature parameter, and l is the number of
315 Sinkhorn iterations. During inference, the logits \mathcal{F} are then directly converted to a hard permutation
316 matrix using the Hungarian algorithm: $\mathbf{P} = \text{Hungarian}\left(-\frac{\mathcal{F} + \gamma \times \text{Gumbel noise}}{\tau}\right)$.
317

318 **Search with Clique-oriented Ordering** After obtaining the hard permutation matrix \mathbf{P} , we reorder
319 the vertices according to this permutation to build what we refer to as the learned *clique-oriented*
320 vertex ordering.
321

322 To enhance MaxCliqueDyn's efficiency, we propose replacing the traditional degree-based ordering
323 (line 3 in Algorithm 1) with our clique-oriented vertex ordering learned through UL. To maintain BnB
324 correctness, we follow Konc and Janezic (2007); Tomita and Seki (2003) by coloring the first $\Delta(G)$
325

¹Our Gumbel-Sinkhorn implementation can use PyTorch's GPU-accelerated tensor operations together with `torch.compile`, which significantly speeds up both the forward optimization and the backward gradient computations in practice.

324 vertices with unique colors from 1 to $\Delta(G)$ and assigning all remaining vertices color $\Delta(G) + 1$.
 325 Since MaxCliqueDyn selects vertices with the highest color label first, this ordering means non-clique
 326 vertices are evaluated earlier in the search process, allowing the algorithm to establish good candidate
 327 cliques during initial phases. These discovered cliques then serve as effective lower bounds as the
 328 search progresses to the potential clique vertices later in the sequence, enabling more aggressive
 329 pruning of the search space, thus leading to fewer total steps and faster execution.

330 In practice, we observe that although the subsequent `ColorSort` procedure in MaxCliqueDyn
 331 will modify the initial vertex ordering, the vertices with maximum colors $C(p)$ (which are selected
 332 for subsequent procedures) tend to maintain a strong correlation with their initial positions in our
 333 clique-oriented ordering. This means that vertices that we initially identified as likely clique members,
 334 despite being reordered by `ColorSort` and $R \cap \Gamma(p)$, still tend to be processed later in the search
 335 process, where $\Gamma(p)$ denotes the neighborhood of vertex p . This delayed processing of potential
 336 clique vertices aligns with our original strategy. Thus, the benefits of our clique-oriented ordering
 337 persist.

338

339 4 EXPERIMENTS

340

341 **Training** Our dataset consists of Erdős-Renyi (ER) graphs with sizes $n \in \{100, 200\}$ and edge
 342 probabilities $p \in \{0.1, 0.2, \dots, 0.9\}$. For each combination of size and probability, we generate
 343 50,000 training graphs, 10,000 validation graphs, and 10,000 test graphs. We train our GNN using
 344 the Adam optimizer with learning rate 0.0001 for 100 epochs per graph configuration. The model
 345 architecture uses a two-layer Scattering Attention GNN (SAG) Min et al. (2022) with 6 scattering
 346 and 3 low-pass channels, with hidden dimension 128 for $n = 100$ and 256 for $n = 200$. The tanh
 347 scale is set to $\alpha = 40$. We conducted experiments using a NVIDIA H100 Graphics Processing Unit
 348 (GPU) and an Intel Xeon Gold 6154 Central Processing Unit (CPU).

349

350 Table 1: Comparison of MaxCliqueDyn with three orderings (Random, Clique-oriented, and Degree
 351 Sort) on random graphs with $n = 10,000$ vertices and varying edge probabilities p . **We use a 5:1:1**
 352 **split for training, validation, and test, and each reported value is the average over 10,000 random**
 353 **instances.** We report the number of steps and computation time (in seconds) for each algorithm. The
 354 Clique-oriented approach includes an additional inference overhead. The maximum clique size ω is
 355 reported in the last column.

p	Random			Clique-oriented			Degree Sort		
	Steps	Time (s)		Steps	Time	Inference (s)	Steps	Time (s)	ω
0.1	94.25	7.799e-5	97.22	<u>7.290e-5</u>	6.357e-5 + 9.424e-4		98.45	7.321e-5	3.962
0.2	110.9	9.900e-5	107.8	9.663e-5	6.323e-5 + 1.030e-3		108.6	<u>9.437e-5</u>	5.022
0.3	159.0	1.480e-4	139.7	<u>1.330e-4</u>	6.402e-5 + 9.302e-4		143.6	1.380e-4	6.122
0.4	284.7	2.565e-4	245.7	<u>2.192e-4</u>	6.379e-5 + 7.107e-4		252.4	2.296e-4	7.514
0.5	535.1	5.042e-4	434.3	<u>3.973e-4</u>	6.345e-5 + 8.736e-4		456.2	4.053e-4	9.191
0.6	973.8	9.766e-4	873.0	<u>8.038e-4</u>	6.371e-5 + 7.767e-4		912.0	8.087e-4	11.45
0.7	1968	1.922e-3	1764	1.625e-3	6.427e-5 + 8.173e-4		1792	<u>1.612e-3</u>	14.65
0.8	4641	5.201e-3	3904	<u>4.200e-3</u>	6.550e-5 + 8.862e-4		4066	4.230e-3	19.86
0.9	4870	7.752e-3	4069	<u>6.118e-3</u>	6.352e-5 + 1.051e-3		4209	6.206e-3	30.69

367
 368 In our experiments on $n = 100$, we vary the temperature parameter $\tau \in \{1, 2, 3, 4, 5\}$ and the noise
 369 scale $\gamma \in \{0.01, 0.02, 0.03, 0.04, 0.05\}$, while fixing $\epsilon = 0.2$ and $l = 20$ for all edge probabilities;
 370 on $n = 200$, we use the same variations for τ and γ , but set ϵ to either 0.06 or $\epsilon = 0.08$, with $l = 10$
 371 for all edge probabilities. We then select the model with fastest inference time on the validation set.
 372 The results on the test data are shown in Table 1 and 2.

373 The best performance is highlighted in bold for the number of steps and underlined for computation
 374 time (excluding inference overhead). For $n = 100$, our learned clique-oriented approach achieves the
 375 lowest number of steps for all edge probabilities except $p = 0.1$, where random ordering performs
 376 marginally better. The reduction in steps becomes more pronounced as edge probability increases,
 377 with up to 16.4% fewer steps compared to random ordering at $p = 0.9$. Our learned clique-oriented
 378 approach achieves the fastest execution in 7 out of 9 cases, while degree-based ordering performs

378
 379 Table 2: Comparison of MaxCliqueDyn with three orderings (Random, Clique-oriented, and Degree
 380 Sort) on random graphs with $n = 200$ vertices and varying edge probabilities p . **We use a 5:1:1**
 381 **split for training, validation, and test, and each reported value is the average over 10,000 random**
 382 **instances.** We report the number of steps and computation time (in seconds) for each algorithm. The
 383 Clique-oriented approach includes an additional inference overhead. The maximum clique size ω is
 384 reported in the last column.

p	Random		Clique-oriented			Degree Sort		
	Steps	Time (s)	Steps	Time (s)	Inference (s)	Steps	Time (s)	ω
0.1	2.040e+2	<u>2.301e-4</u>	2.001e+2	2.306e-4	<u>8.138e-5</u> +5.285e-3	2.031e+2	2.398e-4	4.209
0.2	3.505e+2	3.645e-4	3.236e+2	<u>3.551e-4</u>	<u>8.143e-5</u> +5.588e-3	3.270e+2	3.635e-4	5.881
0.3	9.182e+2	8.213e-4	8.426e+2	<u>7.441e-4</u>	<u>8.100e-5</u> +3.840e-3	8.554e+2	7.536e-4	7.096
0.4	2.196e+3	2.472e-3	2.115e+3	2.306e-3	<u>8.289e-5</u> +5.446e-3	2.220e+3	<u>2.257e-3</u>	8.959
0.5	6.492e+3	8.260e-3	6.119e+3	<u>7.427e-3</u>	<u>8.097e-5</u> +5.309e-3	6.233e+3	7.455e-3	11.02
0.6	2.818e+4	3.692e-2	2.651e+4	<u>3.270e-2</u>	<u>8.133e-5</u> +4.527e-3	2.703e+4	3.281e-2	13.88
0.7	1.372e+5	1.934e-1	1.277e+5	<u>1.717e-1</u>	<u>8.143e-5</u> +6.426e-3	1.299e+5	1.729e-1	18.05
0.8	1.288e+6	2.199e+0	1.182e+6	<u>1.948e+0</u>	<u>8.191e-5</u> +6.146e-3	1.248e+6	2.001e+0	25.20
0.9	1.435e+7	4.076e+1	1.209e+7	<u>3.274e+1</u>	<u>8.132e-5</u> +5.250e-3	1.252e+7	3.360e+1	41.27

397
 398 best in 2 cases ($p = 0.2$ and $p = 0.7$). The time savings correlate strongly with the reduction
 399 in steps. The clique-oriented method does incur an additional inference cost, consisting of two
 400 components: GNN inference ($\approx 6.4 \times 10^{-5}$ seconds) and building a hard permutation using the
 401 Hungarian algorithm ($\approx 9.0 \times 10^{-4}$ seconds). As the edge probability increases from 0.1 to 0.9, all
 402 methods show exponential growth in both steps and computation time. However, the clique-oriented
 403 approach maintains its relative advantage, with the benefits becoming more significant for denser
 404 graphs. To investigate how our method scales with graph size, we conducted additional experiments
 405 on larger graphs with $n = 200$ vertices, with results shown in Table 2.

406 The performance advantage of the clique-oriented ordering becomes more pronounced as both graph
 407 size and density increase. In larger graphs with $n = 200$ vertices, the results are shown in Table 2. Our
 408 clique-oriented ordering consistently achieves the lowest number of steps across all edge probabilities,
 409 with improvements becoming particularly significant on denser graphs. For sparse graphs ($p = 0.1$),
 410 the clique-oriented approach shows a modest improvement, reducing steps by 1.9% compared to
 411 random ordering (from 2.040×10^2 to 2.001×10^2). This advantage over random ordering grows
 412 substantially with edge probability: at $p = 0.6$, steps are reduced by 5.9% (from 2.818×10^4 to
 413 2.651×10^4), and at $p = 0.9$, the improvement reaches 15.7% (from 1.435×10^7 to 1.209×10^7).
 414 Compared with degree-based ordering, the clique-oriented approach reduces 1.9% at $p = 0.6$ and
 415 3.4% at $p = 0.9$. The computation time shows similar trends, with the clique-oriented approach
 416 achieving the fastest execution (excluding inference overhead) in 7 out of 9 cases. The time savings
 417 become most significant on dense graphs. This substantial improvement more than compensates
 418 for the small, constant inference overhead—approximately 8.1×10^{-5} seconds for neural network
 419 inference plus 5.3×10^{-3} seconds for permutation computation.

420 It should be noted that, at $p = 0.8$ and $p = 0.9$, even when including the inference time overhead,
 421 our clique-oriented ordering achieves lower total computation time compared to degree-based sorting.
 422 Specifically, on $p = 0.9$, when we run the inference on our CPU (Intel Xeon Gold 6154), it has an
 423 average inference time of ≈ 0.04 seconds, making total execution time for clique-oriented ordering
 424 at $p = 0.9$ approximately 32.7 seconds, while degree-sort ordering takes 33.6 seconds, resulting in a
 425 2.6% improvement. This demonstrates that even in a CPU-only environment, our clique-oriented
 426 ordering outperforms degree-based ordering. This advantage becomes more pronounced as graph
 427 size and density increase, making our method of great practical value. Our results suggest that our
 428 UL model successfully captures important structural information that guides more efficient BnB.

429 5 THE LEARNED CLIQUE-ORIENTED ORDERING

430 To visualize our UL clique-oriented ordering, we select a randomly generated test instance with
 431 $n = 200$ vertices and edge probability $p = 0.8$. Figure 4 illustrates different vertex ordering

approaches. The random ordering does not show discernible patterns, making it difficult to identify structural properties. Both the clique-oriented and degree-sorted ordering show a concentration of edges in the upper-left region, but with distinct characteristics. The clique-oriented ordering groups clique members together, revealing dense blocks that correspond to strongly connected subgraphs. In contrast, the degree-sorted ordering emphasizes hub-like nodes but makes clique structures less distinguishable, resulting in less distinct dense blocks.

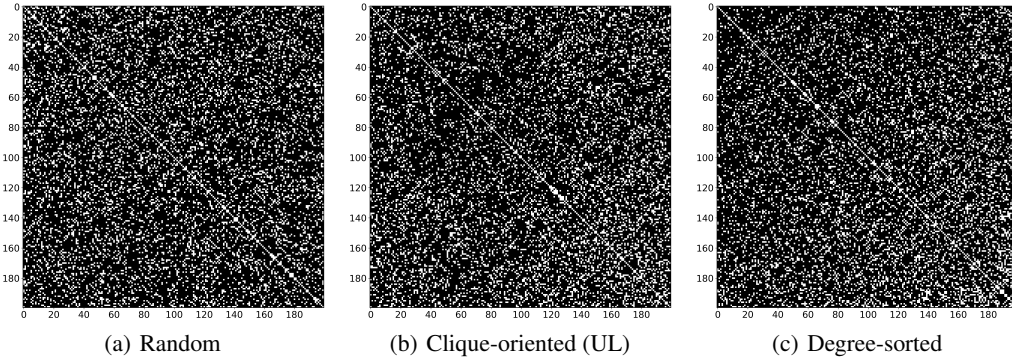


Figure 4: Adjacency matrix visualization of the graph: (a) random ordering, (b) clique-oriented ordering, and (c) matrix sorted by non-increasing degree.

Figure 5 shows adjacency matrices for the first 50 vertices, highlighting cliques of size ≥ 5 . The random ordering (a) exhibits minimal clique structures, while both clique-oriented (b) and degree-sorted (c) orderings effectively cluster vertices belonging to cliques. The clique-oriented ordering demonstrates better clique identification, revealing 7 distinct cliques compared to 6 in the degree-sorted ordering, with cliques positioned closer to the upper-left corner. This validates the effectiveness of our UL approach in revealing inherent clique structures through reordering.

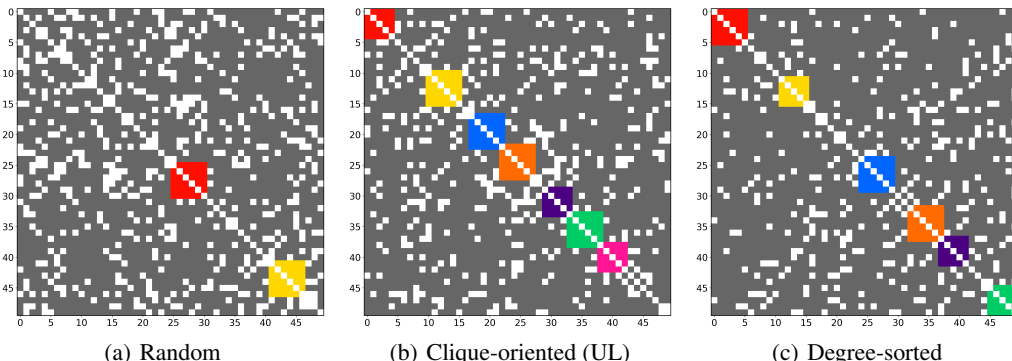


Figure 5: Adjacency matrix of the first 50 nodes of the graph: (a) random ordering, (b) clique-oriented ordering, and (c) matrix sorted by non-increasing degree.

These visual results clearly reflect the goal of our method. The Chebyshev-inspired distance matrix $\mathbf{D}_{\text{Clique}}$ encourages the model to pull likely clique-forming vertex pairs toward the top-left corner, and during training it naturally learns to group densely connected vertices together. The dense blocks that appear in the clique-oriented ordering are therefore a direct outcome of this objective, showing that the model is uncovering meaningful structure rather than arranging vertices arbitrarily. This reordering also benefits exact MCP solvers: when clique candidates appear early, the solver can identify a large clique sooner, tighten the initial lower bound, and prune the search space more effectively. In contrast, degree-based sorting provides no explicit structural bias toward clique formation and often scatters true clique vertices.

Although the clique-oriented (UL) ordering and degree-sorted ordering may look similar at a global level, this is expected because both pull well-connected vertices toward the top-left region. The

486 important differences appear in the finer structure. The UL ordering produces sharper, more coherent
487 dense blocks that align more closely with actual clique memberships, as shown in the zoomed-in view
488 of the first 50 nodes, as shown in Figure 5. Degree sorting tends to group high-degree vertices that are
489 not necessarily part of the same clique, leading to more diffuse patterns. This subtle but consistent
490 sharpening of clique-related regions in the UL ordering is what ultimately gives it a performance
491 advantage, allowing the solver to focus on promising regions of the search space earlier and prune
492 more aggressively.

493

494 6 CONCLUSION

495

496 In this paper, we demonstrate that UL can be used for reordering, where the resulting reordering
497 reveals underlying combinatorial structures. Instead of formulating the MCP as a binary classification
498 problem, we encode it using a permutation framework. This approach enables us to learn the ordering
499 of vertices directly, rather than making binary decisions. After decoding the model’s output, the clique
500 structures are naturally revealed. Importantly, reordering and binary classification approaches are
501 not mutually exclusive: while binary classification focuses on direct yes/no decisions about whether
502 nodes belong to the solution, reordering provides a complementary perspective by uncovering the
503 inherent structural relationships between nodes. By integrating both approaches, we can leverage
504 their respective strengths: binary classification’s explicit decision-making and reordering’s ability to
505 capture structural patterns.

506 Our experiments with MaxCliqueDyn demonstrated that traditional degree-based ordering in BnB
507 can be improved through UL approaches. As graph size and density increase, our inference overhead
508 becomes proportionally smaller in the total execution time. Notably, on the largest, densest graphs
509 ($n = 200, p = 0.9$), our approach outperforms degree-based ordering even when accounting for in-
510 ference time. This demonstrates the practical viability of our UL method, particularly for challenging
511 instances. Given that MaxCliqueDyn is a representative BnB algorithm and degree-based ordering
512 is widely used in most exact clique solvers, these results suggest the potential for improving exact
513 solvers through learned ordering strategies. In this paper, we only replaced the initial degree-based or-
514 dering with our learned clique-oriented ordering. There remain many promising directions for further
515 incorporating clique-oriented ordering into existing algorithms, such as exploring deeper integration
516 of learned clique-oriented methods throughout the search process, beyond just initialization.

517

518 **Sensitivity to Hyperparameters.** We examined how different hyperparameters affect performance
519 and found the model to be generally robust. Increasing the GNN from 2 to 3 layers still improves
520 MaxCliqueDyn, achieving 1.232×10^7 steps and 33.01 seconds on ($n = 200, p = 0.9$) compared
521 to 1.252×10^7 steps and 33.60 seconds. Gumbel noise has only a minor effect, with noise levels
522 of 0.01 and 0.05 both yielding about a 2.5% runtime reduction. The most sensitive component is
523 the Chebyshev-based matrix $\mathbf{D}_{\text{Clique}}$. Our choice $\mathbf{D}_{\text{Clique}} = (1 + \varepsilon)^{(C_n - n/2)}$ works well for small ε ,
524 while larger values (e.g., $\varepsilon = 0.5$) cause numerical instability and degrade performance. This can
525 be mitigated by using smaller ε or a slower-growing polynomial form, as long as weights increase
526 toward the top-left to promote clique formation.

527

528 **Discussion and Future Work.** In this work, we demonstrate that an unsupervised learning-based
529 approach can already improve a widely used exact solver through its initial ordering alone. The key
530 point is that our ordering is learned, not hand-crafted, allowing the model to automatically discover
531 structural patterns that traditional heuristics may not be able to capture.

532 We focus on learning effective initial vertex orderings for MaxCliqueDyn, but the idea is not tied
533 to this solver. Since most exact MCP frameworks depend on an initial ordering to guide branching
534 and pruning, our approach can naturally support many solvers. An important advantage is that the
535 method is fully *unsupervised*, requiring no labels and making it cheap to train and easy to deploy. A
536 supervised variant that learns from high-quality orderings could yield even stronger improvements.
537 Node ordering remains crucial in modern exact MCP algorithms, and a good ordering can serve as
538 a simple yet effective preprocessing step for recent methods as well Li et al. (2013); Li and Quan
539 (2010); San Segundo et al. (2019). Exploring deeper integration between learning and search is a
promising direction for future work.

540 REFERENCES

541

542 Yimeng Min, Yiwei Bai, and Carla P Gomes. Unsupervised learning for solving the travelling
543 salesman problem. *Advances in Neural Information Processing Systems*, 36:47264–47278, 2023.

544 Lars Engebretsen and Jonas Holmerin. Clique is hard to approximate within $n^{1-o(1)}$. In *International*
545 *Colloquium on Automata, Languages, and Programming*, pages 2–12. Springer, 2000.

546 Subhash Khot. Improved inapproximability results for maxclique, chromatic number and approximate
547 graph coloring. In *Proceedings 42nd IEEE Symposium on Foundations of Computer Science*, pages
548 600–609. IEEE, 2001.

549

550 David Zuckerman. Linear degree extractors and the inapproximability of max clique and chromatic
551 number. In *Proceedings of the thirty-eighth annual ACM symposium on Theory of computing*,
552 pages 681–690, 2006.

553

554 Immanuel M Bomze, Marco Budinich, Panos M Pardalos, and Marcello Pelillo. The maximum clique
555 problem. *Handbook of Combinatorial Optimization: Supplement Volume A*, pages 1–74, 1999.

556

557 Etsuji Tomita and Tomokazu Seki. An efficient branch-and-bound algorithm for finding a maximum
558 clique. In *International conference on discrete mathematics and theoretical computer science*,
559 pages 278–289. Springer, 2003.

560

561 Etsuji Tomita, Yoichi Sutani, Takanori Higashi, Shinya Takahashi, and Mitsuo Wakatsuki. A simple
562 and faster branch-and-bound algorithm for finding a maximum clique. In *International Workshop
563 on Algorithms and Computation*, pages 191–203. Springer, 2010.

564

565 Pablo San Segundo, Diego Rodríguez-Losada, and Agustín Jiménez. An exact bit-parallel algorithm
566 for the maximum clique problem. *Computers & Operations Research*, 38(2):571–581, 2011.

567

568 Janez Konc and Dušanka Janezic. An improved branch and bound algorithm for the maximum clique
569 problem. *proteins*, 4(5):590–596, 2007.

570

571 Qinghua Wu and Jin-Kao Hao. A review on algorithms for maximum clique problems. *European
572 Journal of Operational Research*, 242(3):693–709, 2015.

573

574 Nikolaos Karalias and Andreas Loukas. Erdos goes neural: an unsupervised learning framework for
575 combinatorial optimization on graphs. *Advances in Neural Information Processing Systems*, 33:
576 6659–6672, 2020.

577

578 Nikolaos Karalias, Joshua Robinson, Andreas Loukas, and Stefanie Jegelka. Neural set function
579 extensions: Learning with discrete functions in high dimensions. *Advances in Neural Information
580 Processing Systems*, 35:15338–15352, 2022.

581

582 Randy Carraghan and Panos M Pardalos. An exact algorithm for the maximum clique problem.
583 *Operations Research Letters*, 9(6):375–382, 1990.

584

585 Hua Jiang, Chu-Min Li, and Felip Manya. An exact algorithm for the maximum weight clique problem
586 in large graphs. In *Proceedings of the AAAI conference on artificial intelligence*, volume 31, 2017.

587

588 Sándor Szabó and Bogdan Zavalnij. A different approach to maximum clique search. In *2018
589 20th International Symposium on Symbolic and Numeric Algorithms for Scientific Computing
590 (SYNASC)*, pages 310–316. IEEE, 2018.

591

592 Junya Arai, Hiroaki Shiokawa, Takeshi Yamamuro, Makoto Onizuka, and Sotetsu Iwamura. Rabbit
593 order: Just-in-time parallel reordering for fast graph analysis. In *2016 IEEE International Parallel
594 and Distributed Processing Symposium (IPDPS)*, pages 22–31. IEEE, 2016.

595

596 Vignesh Balaji and Brandon Lucia. When is graph reordering an optimization? studying the effect of
597 lightweight graph reordering across applications and input graphs. In *2018 IEEE International
598 Symposium on Workload Characterization (IISWC)*, pages 203–214. IEEE, 2018.

599

600 Nikolai Merkel, Pierre Toussing, Ruben Mayer, and Hans-Arno Jacobsen. Can graph reordering
601 speed up graph neural network training? an experimental study. *arXiv preprint arXiv:2409.11129*,
602 2024.

594 Chu-Min Li, Hua Jiang, and Felip Manyà. On minimization of the number of branches in branch-
595 and-bound algorithms for the maximum clique problem. *Computers & Operations Research*, 84:
596 1–15, 2017.

597 Ciaran McCreesh and Patrick Prosser. Multi-threading a state-of-the-art maximum clique algorithm.
598 *Algorithms*, 6(4):618–635, 2013.

599 Pablo San Segundo, Alvaro Lopez, and Panos M Pardalos. A new exact maximum clique algorithm
600 for large and massive sparse graphs. *Computers & Operations Research*, 66:81–94, 2016.

601 Yimeng Min and Carla Gomes. Unsupervised learning permutations for tsp using gumbel-sinkhorn
602 operator. In *NeurIPS 2023 Workshop Optimal Transport and Machine Learning*, 2023.

603 Chu-Min Li and Zhe Quan. Combining graph structure exploitation and propositional reasoning for
604 the maximum clique problem. In *2010 22nd IEEE international conference on tools with artificial
605 intelligence*, volume 1, pages 344–351. IEEE, 2010.

606 Gonzalo Mena, David Belanger, Scott Linderman, and Jasper Snoek. Learning latent permutations
607 with gumbel-sinkhorn networks. In *International Conference on Learning Representations*, 2018.

608 Yimeng Min, Frederik Wenkel, Michael Perlmutter, and Guy Wolf. Can hybrid geometric scattering
609 networks help solve the maximum clique problem? *Advances in Neural Information Processing
610 Systems*, 35:22713–22724, 2022.

611 Chu-Min Li, Zhiwen Fang, and Ke Xu. Combining maxsat reasoning and incremental upper bound
612 for the maximum clique problem. In *2013 IEEE 25th international conference on tools with
613 artificial intelligence*, pages 939–946. IEEE, 2013.

614 Pablo San Segundo, Fabio Furini, and Jorge Artieda. A new branch-and-bound algorithm for the
615 maximum weighted clique problem. *Computers & Operations Research*, 110:18–33, 2019.

616 Ivan Karpukhin, Foma Shipilov, and Andrey Savchenko. Hotpp benchmark: Are we good at the long
617 horizon events forecasting? *arXiv preprint arXiv:2406.14341*, 2024.

618
619
620
621
622
623
624
625
626
627
628
629
630
631
632
633
634
635
636
637
638
639
640
641
642
643
644
645
646
647

648 A COMPUTE THE HARD PERMUTATION

649
 650 In our implementation, we use `scipy.optimize.linear_sum_assignment` to compute the
 651 final hard permutation. We also tested the open-source CUDA batched assignment solver from
 652 Karpukhin et al. (2024), which substantially speeds up hard-permutation decoding when using large
 653 batch sizes.

654 B GENERALIZATION

655 To investigate our model's capability to handle varying graph dimensions, we employ a zero-padding
 656 strategy for size generalization. Given a graph with $n = 190$ nodes and edge probability $p = 0.9$,
 657 we pad it with 10 dummy nodes to match our training dimension. To ensure similar edge density
 658 between training and testing graphs after padding, we train the model on ER random graphs with
 659 $n = 200$ nodes and edge probability $p = 0.81$. Specifically, these dummy nodes have zero feature
 660 vectors, and their corresponding entries in the adjacency matrix are also set to zero, making them
 661 isolated nodes. This padding strategy provides a general approach to handle size differences: smaller
 662 graphs can be padded to the larger sizes, enabling our model to process arbitrary sizes.

663
 664 Table 3: Comparison of MaxCliqueDyn with three orderings (Random, Generalized Clique-oriented,
 665 and Degree Sort) on random graphs with $n = 190$ vertices and edge probabilities $p = 0.9$. For each
 666 algorithm, we report the number of steps taken and computation time in seconds. The size of the
 667 largest clique found ω is shown in the rightmost column.

p	Random		Generalized Clique-oriented			Degree Sort		ω
	Steps	Time (s)	Steps	Time (s)	Inference (s)	Steps	Time (s)	
0.9	7.145e+6	1.923e+1	5.656e+6	1.476e+1	8.191e-5+6.146e-3	5.886e+6	1.523e+1	40.46

668
 669 We use the same training method described in Section 4 and our results are shown in Table 3.
 670 The generalized clique-oriented model performs effectively, requiring 5.656×10^6 steps and 14.76
 671 seconds to find the maximum clique in an ER random graph with $n = 190$ and $p = 0.9$. This result
 672 outperforms both the random algorithm (7.145×10^6 steps, 19.23 seconds) and the degree sort method
 673 (5.886×10^6 steps, 15.23 seconds). The additional inference overhead of our method (approximately
 674 6.23 milliseconds) is negligible compared to the overall computation time, demonstrating that our
 675 generalized approach maintains efficiency while handling different sizes.

676 C PROOF

677 The following proof discusses the connection between the Chebyshev distance complement $\overline{C_n}$ in
 678 exponential form and the maximum clique problem. Specifically,

679 **Lemma 1.** *When $\mathbf{D}_{\text{Clique}} = (n^2)^{\overline{C_n}}$ with $\overline{C_n}[i, j] = n - \max(i, j)$, minimizing $\mathcal{L}_{\text{clique}}(P) =$
 680 $\langle P^T(J - I - A)P, \mathbf{D}_{\text{Clique}} \rangle$ yields the maximum clique.*

681 *Proof.* Let $G = (V, E)$ be an undirected graph with adjacency matrix A . The matrix $J - I - A$
 682 represents non-adjacent vertex pairs, where $J \in \mathbb{R}^{n \times n}$ is the all-ones matrix and $I \in \mathbb{R}^{n \times n}$ is the
 683 identity matrix.

684 Let ω be the size of the maximum clique in G . We will show that any permutation matrix that
 685 minimizes $\mathcal{L}_{\text{clique}}(P)$ must place the maximum clique in the first ω positions.

686 Let P_1 be a permutation matrix that places a maximum clique of size ω in the first ω positions. The
 687 corresponding cost is:

$$688 \mathcal{L}_{\text{clique}}(P_1) = \sum_{i=1}^n \sum_{j=1}^n [P_1^T(J - I - A)P_1]_{ij} \cdot (n^2)^{n - \max(i, j)} \quad (6)$$

702 Since the first ω vertices form a clique, we have $[P_1^T(J - I - A)P_1]_{ij} = 0$ for all $1 \leq i, j \leq \omega$.
 703 Non-adjacent vertex pairs can only exist in positions where at least one index exceeds ω . For these
 704 positions, we have $n - \max(i, j) \leq n - (\omega + 1) = n - \omega - 1$. Therefore:
 705

706

$$\mathcal{L}_{\text{clique}}(P_1) \leq \sum_{\substack{i,j \\ \max(i,j) > \omega}} [P_1^T(J - I - A)P_1]_{ij} \cdot (n^2)^{n-\max(i,j)} \quad (7)$$

707

$$\leq \sum_{\substack{i,j \\ \max(i,j) > \omega}} (n^2)^{n-\max(i,j)} \quad (8)$$

708

$$\leq (n^2 - \omega^2) \cdot (n^2)^{n-\omega-1} \quad (9)$$

715 Now, let P_2 be any permutation matrix that does not place the maximum clique in the first ω positions.
 716 Then at least one vertex from the maximum clique must be placed at position $\omega + 1$ or beyond, and at
 717 least one non-clique vertex must be placed among the first ω positions.

718 Since the first ω positions cannot contain only clique vertices, there must exist at least one pair of
 719 vertices in the first ω positions that are not adjacent. This non-adjacent pair contributes a value of
 720 1 to $[P_2^T(J - I - A)P_2]_{ij}$ where $\max(i, j) \leq \omega$. The corresponding weight is at least $(n^2)^{n-\omega}$.
 721 Therefore:

722

$$\mathcal{L}_{\text{clique}}(P_2) \geq (n^2)^{n-\omega} \quad (10)$$

723 We can now directly compare the bounds:

724

$$\frac{\mathcal{L}_{\text{clique}}(P_1)}{\mathcal{L}_{\text{clique}}(P_2)} \leq \frac{(n^2 - \omega^2) \cdot (n^2)^{n-\omega-1}}{(n^2)^{n-\omega}} \quad (11)$$

725

$$= \frac{n^2 - \omega^2}{n^2} \quad (12)$$

726

$$= 1 - \frac{\omega^2}{n^2} < 1 \quad (13)$$

727 This implies $\mathcal{L}_{\text{clique}}(P_1) < \mathcal{L}_{\text{clique}}(P_2)$ for any permutation P_2 that does not place the maximum
 728 clique in the first ω positions. Therefore, any permutation matrix that minimizes $\mathcal{L}_{\text{clique}}(P)$ must
 729 place the maximum clique in the first ω positions. \square

730
 731
 732
 733
 734
 735
 736
 737
 738
 739
 740
 741
 742
 743
 744
 745
 746
 747
 748
 749
 750
 751
 752
 753
 754
 755